

## Negative shock waves

By P. A. THOMPSON AND K. C. LAMBRAKIS

Division of Fluid, Chemical and Thermal Processes, Rensselaer Polytechnic Institute,  
Troy, New York

(Received 15 November 1972 and in revised form 11 April 1973)

Negative or rarefaction shock waves may exist in single-phase fluids under certain conditions. It is necessary that a particular fluid thermodynamic quantity  $\Gamma \equiv -\frac{1}{2}\partial \ln(\partial P/\partial \nu)_s/\partial \ln \nu$  be negative: this condition appears to be met for sufficiently large specific heat, corresponding to a sufficient level of molecular complexity. The dynamic formation and evolution of a negative shock is treated, as well as its properties. Such shocks satisfy stability conditions and have a positive, though small, entropy jump. The viscous shock structure is found from an approximate continuum model. Possible experimental difficulties in the laboratory production of negative shocks are briefly discussed.

### 1. Introduction

A negative or rarefaction shock wave is distinguished by having a negative pressure jump across it,  $[P] < 0$ . The possibility of such shocks will be associated with negative values of the thermodynamic quantity  $(\partial^2 P/\partial \nu^2)_s$ ,

$$(\partial^2 P/\partial \nu^2)_s < 0, \quad (1.1)$$

where  $P$  is the pressure,  $\nu$  specific volume and  $s$  specific entropy. The requirement (1.1) is the reversed form of the inequality usually assumed in the analysis of shock wave properties, for example, by Hayes (1958).

The derivative in (1.1) is more conveniently expressed in the non-dimensional form

$$\Gamma \equiv -\frac{\nu}{2} \left( \frac{\partial^2 P}{\partial \nu^2} \right)_s / \left( \frac{\partial P}{\partial \nu} \right)_s, \quad (1.2)$$

which necessarily has the sign of  $(\partial^2 P/\partial \nu^2)_s$ , because  $(\partial P/\partial \nu)_s < 0$  from the requirement for thermodynamic stability. The sign of  $\Gamma$  is therefore geometrically associated with the curvature of an isentrope in the  $P, \nu$  plane, and  $\Gamma < 0$  is equivalent to (1.1). Because  $\Gamma$  plays a crucial role in determining *nonlinear* gasdynamic behaviour, we refer to it as the *fundamental derivative*.

We briefly trace the history of negative shocks. The development of arguments against these peculiar shock waves is reminiscent of the history of shock waves in general, especially because proofs of impossibility have been widely accepted in both cases. Negative shocks were first ruled out in a footnote of the celebrated paper of Rankine (1870), viz. "Sir William Thomson [Lord Kelvin] has pointed out to the author that a wave of sudden rarefaction, though mathematically

possible, is an unstable condition of motion . . .". More formally, Jouguet (1901), Zemplén (1905) and Rayleigh (1910) showed impossibility for a perfect gas on the basis that the requirement  $[s] \geq 0$  is violated. We note that Zemplén originated the distinctive terms *positive* shock and *negative* shock, which we prefer to the corresponding 'compression' and 'rarefaction' terminology.

Duhem (1909) first showed the association of  $\Gamma > 0$  with positive shocks and  $\Gamma < 0$  with negative shocks, for arbitrary equations of state, though he did not explicitly put his result in those terms.

The important work of Bethe (1942), never published in a scientific journal, yields pertinent results, including the well-known formula for weak shocks

$$T_1[s] = -\frac{1}{12}(\partial^2 P/\partial v^2)_s [\nu]^3 + O([\nu]^4). \quad (1.3)$$

From elementary shock theory,  $-[P]/[\nu]$  is the square of the mass flux across the shock front. Thus  $[P]$  and  $[\nu]$  necessarily have opposite signs, and this formula shows that  $[s] > 0$  is satisfied if  $\Gamma > 0$  and  $[P] > 0$  (positive shock) or if  $\Gamma < 0$  and  $[P] < 0$  (negative shock), provided that  $[P]$  is sufficiently small. Bethe actually investigated the possibility that  $\Gamma < 0$  and found two significant results: first, that  $\Gamma < 0$  within a certain region for a van der Waals gas if  $c_v/R > 17.5$  and second, that  $\Gamma = \pm \infty$  at the vapour/mixture phase boundary, where the plus sign applies to a fluid which tends to condense on isentropic expansion and the negative sign applies to a fluid which tends to evaporate on isentropic expansion (retrograde fluid). But Bethe dismissed either behaviour leading to  $\Gamma < 0$  on the basis of (incorrect) physical arguments.

Zel'dovich (1946), again using a van der Waals gas model, found a negative- $\Gamma$  region in the vapour phase for substances with  $c_v/R \gtrsim 10$ . Zel'dovich & Raizer (1966) briefly discuss the possibility of negative shocks in a  $\Gamma < 0$  vapour region and mention that such shocks may satisfy the condition  $[s] > 0$ . In addition, Zel'dovich & Raizer (1967) discuss negative shocks at a phase boundary where  $\Gamma = -\infty$  (i.e. where the slope of the isentrope is discontinuous), with particular reference to solids.

In the present paper we set out to determine whether or not negative shocks can in fact exist in real fluids, in the vapour phase in particular, and finding their existence, to predict their behaviour from continuum theory. To do this it is first of all necessary to find  $\Gamma < 0$  regions for real fluids, that is, fluids accessible to experiments.

## 2. The fundamental derivative $\Gamma$

The importance of  $\Gamma$  in the determination of various forms of gasdynamic behaviour has been discussed by Thompson (1971). In the present context, its *sign* will admit or deny the possibility of negative shocks; its *magnitude* will determine their behaviour.

The sound speed  $c$  is defined by

$$c^2 = -\nu^2(\partial P/\partial \nu)_s > 0. \quad (2.1)$$

From the definition (1.2) the following identities can be obtained by thermodynamic manipulation:

$$\Gamma = \frac{c^4}{2\nu^3} \left( \frac{\partial^2 \nu}{\partial P^2} \right)_s = \frac{\nu^3}{2c^2} \left( \frac{\partial^2 P}{\partial \nu^2} \right)_s = c \left( \frac{\partial(\rho c)}{\partial P} \right)_s, \quad (2.2)$$

$$2\Gamma = \{\partial(P + \rho c^2)/\partial P\}_s, \quad (2.3)$$

$$\Gamma - 1 = \rho c(\partial c/\partial P)_s. \quad (2.4)$$

These identities will be useful in the calculation of shock wave behaviour. The last form of (2.2) is essentially that of Hayes (1958), whom we have followed in using the symbol  $\Gamma$  for the fundamental derivative.

For a perfect gas with ratio of specific heats  $\gamma$  one finds from (2.2) that  $\Gamma = \frac{1}{2}(\gamma + 1)$ , of order unity. For typical liquids  $\Gamma$  is in the range 4–6 (Thompson 1971). To investigate conditions intermediate between the dilute-gas and liquid states it is helpful to have a general expression for finding  $\Gamma$  from conventional thermodynamic information. We make use of a formula given by Bethe, written in the non-dimensional form

$$\begin{aligned} \left( \frac{\partial^2 \hat{P}}{\partial \hat{v}^2} \right)_s = & \left( \frac{\partial^2 \hat{P}}{\partial \hat{v}^2} \right)_T - 3Z_c \epsilon \hat{T} \left( \frac{\partial \hat{P}}{\partial \hat{T}} \right)_\nu \frac{\partial^2 \hat{P}}{\partial \hat{v} \partial \hat{T}} + 3Z_c^2 \epsilon^2 \hat{T}^2 \left( \frac{\partial \hat{P}}{\partial \hat{T}} \right)_\nu^2 \left( \frac{\partial^2 \hat{P}}{\partial \hat{T}^2} \right)_\nu \\ & + Z_c^2 \epsilon^2 \hat{T} \left( \frac{\partial \hat{P}}{\partial \hat{T}} \right)_\nu^3 \left\{ 1 - \frac{\hat{T}}{c_\nu} \left( \frac{\partial c_\nu}{\partial \hat{T}} \right)_\nu \right\} \end{aligned} \quad (2.5)$$

and 
$$\left( \frac{\partial \hat{P}}{\partial \hat{v}} \right)_s = \left( \frac{\partial \hat{P}}{\partial \hat{v}} \right)_T - Z_c \epsilon \hat{T} \left( \frac{\partial \hat{P}}{\partial \hat{T}} \right)_\nu^2, \quad (2.6)$$

where  $\hat{P}$ ,  $\hat{v}$  and  $\hat{T}$  are reduced pressure, volume and temperature,  $c_\nu$  is constant-volume specific heat,  $Z_c$  is the critical compressibility factor and  $\epsilon \equiv R/c_\nu$  is the (inverse) non-dimensional specific heat. By making use of the identity

$$(\partial c_\nu / \partial \nu)_T = T(\partial^2 P / \partial T^2)_\nu,$$

the specific heat can be written as

$$\frac{c_\nu}{R} = \frac{c_\nu^0(\hat{T})}{R} + Z_\nu \hat{T} \int_\infty^{\hat{v}} \left( \frac{\partial^2 \hat{P}}{\partial \hat{T}^2} \right)_\nu d\hat{v}, \quad (2.7)$$

For a substance with a known thermal equation of state  $\hat{P} = f(\hat{v}, \hat{T})$  and known  $c_\nu^0(T)$ , the formulae (2.5)–(2.7) allow calculation of  $\Gamma$  from its definition (1.2).

A useful idealization is the *law of corresponding states*, according to which there is a universal function  $\hat{P}(\hat{v}, \hat{T})$ , valid for all substances, and  $Z_c$  is a universal constant (e.g.  $Z_c = 0.27$ ). If this law holds, it is a formal consequence of (2.5)–(2.7) that

$$\Gamma = \Gamma(\hat{v}, \hat{T}, \epsilon^0(\hat{T})), \quad (2.8)$$

i.e., at fixed volume and temperature, the value of  $\Gamma$  depends only on the (non-dimensional) zero-pressure specific heat of the substance under consideration. Although this conclusion is based on an idealization, the essential result that  $\Gamma$  correlates with the zero-pressure specific heat will prove useful.

### 3. On possible states with $\Gamma < 0$

To discuss the sign of  $\Gamma$ , it is sufficient to fix attention on (2.5), i.e. the numerator in the expression for  $\Gamma$ . The dominant negative term in (2.5) is the first on the right-hand side, corresponding to the well-known reversed curvature of isotherms in the  $P, \nu$  plane to the right of the critical point. We shall find that  $\Gamma < 0$  in this general region provided that the remaining terms can be made sufficiently small, which can be accomplished by making  $\epsilon$  sufficiently small. In particular, the second term on the right-hand side is everywhere positive, and will be the most important of the remaining terms because it carries a coefficient  $\epsilon^1$ , while the later terms have  $\epsilon^2$  coefficients. We thus find that the problem of finding  $\Gamma < 0$  reduces to the problem of finding sufficiently small  $\epsilon = R/c_v$ , i.e. of finding sufficiently large  $c_v/R$ . Note that in the limit as  $\epsilon \rightarrow 0$  (infinite specific heat!) the isotherms and isentropes become coincident, a situation which is nicely expressed by (2.6).

The calculation of  $\Gamma$  requires an explicit  $\hat{P}, \hat{v}, \hat{T}$  equation. The approximation inherent in a universal corresponding states relation  $\hat{P}(\hat{v}, \hat{T})$  can be reduced by including parameters  $\alpha_i$  peculiar to the substance under consideration:

$$\hat{P} = \hat{P}(\hat{v}, \hat{T}, \alpha_1, \alpha_2, \dots, \alpha_n), \quad (3.1)$$

where the  $\alpha$ 's represent non-dimensional parameters such as the critical compressibility  $Z_c$ , the Riedel constant and the acentric factor. Where the number of parameters  $\alpha_i$  is small (zero to two, say) we speak of 'simple' equations of state; where the number of parameters is large, incorporating most of the measurable idiosyncracies of an individual substance, we speak of 'comprehensive' equations of state. We give below results for the simple equations of van der Waals, Redlich & Kwong, Clausius and Abbott, and for the comprehensive equations of Hirschfelder *et al.* and Martin & Hou. For the simple equations  $c_v^0(\hat{T})$  was represented over a restricted temperature range by

$$c_v^0(\hat{T}) = c_v^0(1)\hat{T}^n, \quad (3.2)$$

with  $n \approx 0.75$  for hydrocarbons and  $n \approx 0.45$  for fluorocarbons. For the comprehensive equations, empirical relations from the literature were used for  $c_v^0(T)$ .

#### 3.1. Van der Waals' equation

This is the oldest and simplest of the equations describing both gas and liquid phases: its simplicity is balanced, however, by limited accuracy. To some extent the calculations given here retread ground already covered by Bethe & Placzek (Bethe 1942) and by Zel'dovich (1946), but yield explicit formulae not given by these authors.

In reduced form the van der Waals equation is

$$\hat{P} = 8\hat{T}/(3\hat{v} - 1) - 3/\hat{v}^2, \quad (3.3)$$

from which it follows that  $Z_c = \frac{3}{8}$  and  $c_v = c_v(T)$  only. Substitution into (2.5) and (2.6) yields

$$\Gamma = \frac{3}{2} \left( \frac{\hat{v}}{3\hat{v} - 1} \right) \frac{k(k+1) - n(k-1)^2 - (4\hat{v}\hat{T})^{-1} \{(3\hat{v} - 1)/\hat{v}\}^3}{k - (4\hat{v}\hat{T})^{-1} \{(3\hat{v} - 1)/\hat{v}\}^2}, \quad (3.4)$$

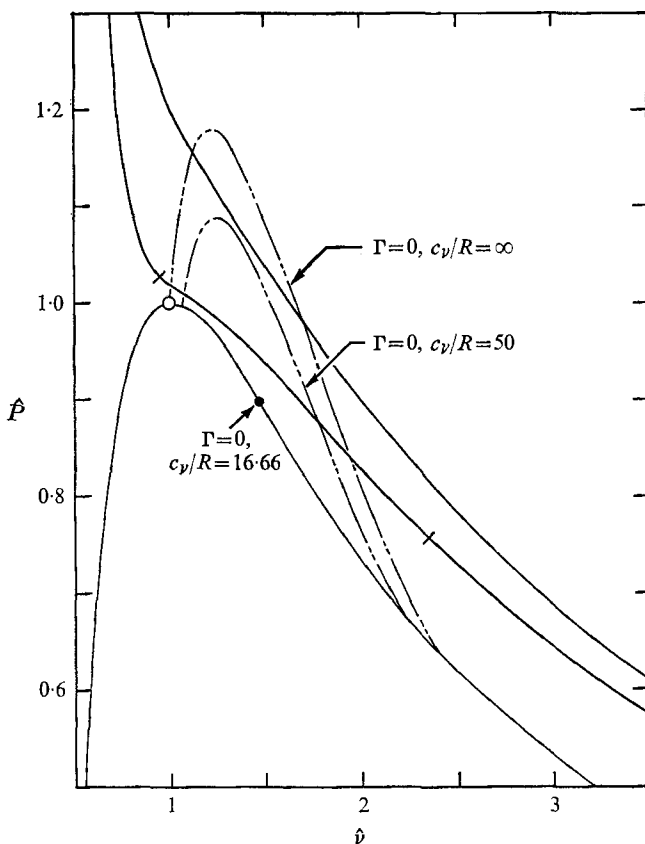


FIGURE 1. Results for a van der Waals substance in the  $\hat{P}$ ,  $\hat{v}$  plane (reduced co-ordinates), showing negative- $\Gamma$  regions for  $c_v^0(T_c)/R = 50$  and  $c_v^0(T_c)/R = \infty$  and two isentropes for the case  $c_v^0(T_c)/R = 50$ .

where  $k \equiv 1 + R/c_v = 1 + \epsilon$  is equal to the ratio of specific heats at zero pressure,  $k = \gamma^0$ . To find the minimum value of  $c_v/R$  leading to  $\Gamma \leq 0$  we find the maximum value of the last term in the numerator of (3.4). This occurs on the saturation line at  $\hat{P} = 0.888$ ,  $\hat{v} = 1.4843$  (not  $\hat{v} = \frac{4}{3}$ , given by Bethe),  $\hat{T} = 0.971$ , and has a value 2.1837; then setting the numerator to zero (i.e.  $\Gamma = 0$ ) yields a quadratic with solution corresponding to the minimum values of  $c_v/R = 1/(k-1)$  for which  $\Gamma = 0$  in the vapour region:

$$(c_v/R)_{\min} = 16.66, 16.50, 16.33 \quad \text{for } n = 0, 0.5, 1.$$

The effect of specific heat variable with temperature is seen to be small.

The  $\Gamma = 0$  locus, bounding the region for which  $\Gamma < 0$ , is found by setting the numerator in (3.4) to zero. With (3.3) this yields

$$\hat{P} = \frac{1}{\hat{v}^2} \left[ \frac{1}{\lambda} \left( \frac{3\hat{v}-1}{\hat{v}} \right)^2 - 3 \right], \tag{3.5}$$

where  $\lambda \equiv \frac{1}{2}\{k(k+1) - n(k-1)^2\}$ . For various values of  $c_v/R = 1/(k-1)$ , the resulting curves are shown in figure 1.

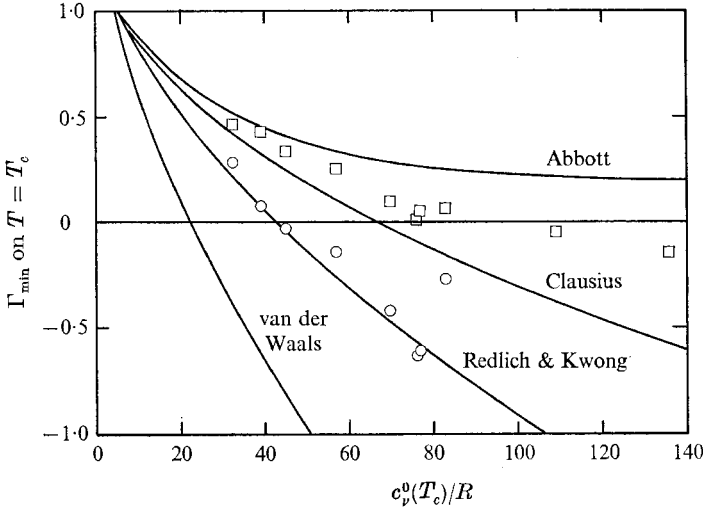


FIGURE 2. The minimum value of  $\Gamma$  along the critical isotherm calculated from various  $P\nu T$  equations.  $\square$ , for various substances, calculated from the equation of Martin & Hou;  $\circ$ , for various substances, calculated from the equation of Hirschfelder *et al.* Values of  $\Gamma$  smaller than those shown are reached on the saturated vapour line.

The van der Waals isentrope can be found by integration of (2.6): with  $k = \text{constant}$ , this yields

$$P = \sigma(s)/(3\hat{v} - 1)^k - 3/\hat{v}^2, \tag{3.6}$$

where  $\sigma(s)$  is a function of the entropy only. Two such isentropes are illustrated in figure 1. We also remark that (3.6) has two degenerate forms: for  $\hat{v} \rightarrow \infty$  it reduces to  $\hat{P}\hat{v}^k = \text{constant}$  (perfect gas, for which case  $k = \gamma$ ) and for  $k = 1$  ( $c_v/R = \infty$ ) it reduces to the expression (3.3) for a van der Waals isotherm.

### 3.2. Other simple equations of state

The  $\hat{P}$ ,  $\hat{v}$ ,  $\hat{T}$  equations of Redlich & Kwong, Clausius and Abbott (Abbott 1973) can be written respectively as

$$\hat{P} = \frac{3\hat{T}}{\hat{v} - B} - \frac{1}{B\hat{T}^{1/2}\hat{v}(\hat{v} + B)}, \tag{3.7}$$

$$\hat{P} = \frac{4\hat{T}}{1 + 4Z_c(\hat{v} - 1)} - \frac{3}{\hat{T}\{1 + \frac{8}{3}Z_c(\hat{v} - 1)\}^2}, \tag{3.8}$$

$$\hat{P} = \frac{12\hat{T}}{4\hat{v} - 1} - \frac{81\{(59 - 5\alpha_c)\hat{T}^{-3/2} + (5\alpha_c - 29)\hat{T}^{-1/2}\}}{10(8\hat{v} + 1)^2}. \tag{3.9}$$

In (3.7), the constant  $B = 2^{1/2} - 1 = 0.25992$ . In (3.8) the critical compressibility factor  $Z_c$  can be arbitrarily chosen: finding the value of  $\Gamma$  to be extremely insensitive to this value, we have used  $Z_c = 0.25$ . In (3.9) the Riedel parameter  $\alpha_c$  (which is the slope of the vapour-pressure curve  $\hat{P}(\hat{T})$  at the critical point) can be arbitrarily chosen: both this parameter and the zero-pressure specific heat  $c_v^0(T_c)$

at the critical temperature increase with molecular complexity and are correlated fairly well by

$$\alpha_c \approx 6 + 0.04 c_p^0(T_c)/R, \quad (3.10)$$

which has been used in the calculation of  $\Gamma$ .

Numerically calculated values of the minimum  $\Gamma$  along the critical isotherm are shown in figure 2, which illustrates the wide variance between different equations of state. We remark that the values shown are larger than the absolute minimum in the vapour region since  $\Gamma$  decreases rapidly toward the saturation curve.

### 3.3. Comprehensive equations of state

Numerical calculations using the equations of Hirschfelder *et al.* (1958) and of Martin & Hou (1955) have been carried out for a large number of substances. The results are shown in figure 2 and a partial listing is given in table 1. Independent calculations by a number of other investigators are reported in Lambrakis & Thompson (1972).

In every case it is found that  $\Gamma$  becomes negative for sufficiently large  $c_p/R$ , i.e. for substances of sufficient molecular complexity.

### 3.4. Remarks on thermodynamic stability

There is no violation of intrinsic thermodynamic stability involved in  $\Gamma < 0$  states. This point has been explicitly treated by Hatsopoulos & Keenan (1965, p. 449).

Whether the equations of state used in calculating  $\Gamma$  satisfy the basic stability requirements  $c_p > 0$  and  $(\partial P/\partial v)_T \leq 0$  is a separate question. All of the equations investigated satisfy  $c_p > 0$ , assuming physically realizable input  $c_p^0 > 0$ . Any  $P, v, T$  equation which predicted  $(\partial P/\partial v)_T > 0$  would be considered bizarre indeed, precautions against such behaviour normally being incorporated into the equation, especially near the critical point.

However, we have recently found that the equation of Hirschfelder *et al.* does predict  $(\partial P/\partial v)_T > 0$  to the right of the critical point for  $Z_c < 0.302$ , the effect becoming somewhat pronounced at  $Z_c \approx 0.25$ . This behaviour exaggerates the reversed curvature of the isotherms and consequently leads to values of  $\Gamma$  which are unrealistically small. On this account we believe that the negative- $\Gamma$  behaviour reported in Lambrakis & Thompson (1972) and shown in figure 2 is too optimistic and that the predictions of the Martin & Hou equation are to be preferred.

## 4. Shock formation from plane waves in unsteady flow

The development of an ordinary positive shock wave from a steepening compression wave is a conventional result in gasdynamics. We now find the corresponding development of a negative shock from a steepening rarefaction wave, which will ensue if some of the thermodynamic states on the rarefaction wave lie within a  $\Gamma < 0$  region. The calculation proceeds according to the gasdynamic theory of simple waves: peculiar features arise from the rapid variation of  $\Gamma$  with pressure which is typical in the neighbourhood of  $\Gamma < 0$  regions.

Formula	Substance	$\bar{M}$	$T_c$ (°K)	$P_c$ (atm)	$Z_c$	$\alpha_c$	$c_p^0(T_c)/R$	$\Gamma_{\min}$ on $T = T_c$		
								HBMS	MH	BWR
$C_6H_{14}$	n-hexane	86.17	508	29.9	0.264	7.27	25.4	0.33	0.55	0.45
$C_7H_{16}$	n-heptane	100.20	540	27.0	0.259	7.53	31.0	0.18	0.48	0.32
$C_8H_{18}$	n-octane	114.22	569	24.6	0.256	7.76	36.8	0.07	0.45	—
$C_9H_{20}$	n-nonane	128.25	595	22.5	0.250	7.94	42.6	-0.10	0.40	—
$C_{10}H_{22}$	n-decane	142.28	618	20.8	0.246	8.18	48.5	-0.27	0.38	-0.40
$C_6F_{14}$	Pf-n-hexane	338.04	451	18.1	0.262	8.08	39.3	0.08	0.43	—
$C_{10}F_{22}$	Pf-n-decane	538.08	578	12.9	0.255	8.2	76	-0.63	0.01	—
$C_7F_{14}$	Pf-methylcyclohexane	350.06	486	19.9	0.266	7.84	45.0	-0.03	0.34	—
$C_8F_{16}$	Pf-1,3-dimethylcyclohexane	400.06	515	18.6	0.267	8.03	69.6	-0.40	0.09	—
$C_{10}F_{18}$	Pf-decalin	462.08	565	17.3	0.262	8.06	67.8	-0.45	—	—
$C_{11}F_{20}$	Pf-methyldecalin	512.09	587	16.4	0.261	8.07	76.6	-0.61	0.05	—
$C_8F_{16}O$	Pf-2-butyltetrahydrofuran	416.06	501	15.8	0.264	8.38	38.2	0.14	0.47	—
$C_8F_{17}HO_2$	Fluorinated ether E-2	452.08	491	13.5	0.263	9.50	57.0	-0.14	0.25	—
$C_{11}F_{23}HO_3$	Fluorinated ether E-3	618.12	536	10.7	0.254	9.98	82.9	-0.27	0.06	—
$C_{14}F_{29}HO_4$	Fluorinated ether E-4	784.15	568	8.31	0.245	10.50	109.0	-1.29	-0.05	—
$C_{17}F_{35}HO_5$	Fluorinated ether E-5	950.18	595	7.6	0.239	10.97	135.7	-2.54	-0.15	—

TABLE 1. Values of the zero-pressure specific heat  $c_p^0/R$  at the critical temperature and other relevant parameters for various substances. Most of the substances were chosen for inclusion on the basis of availability, stability and large specific heat. The tabulated values of  $\Gamma_{\min}$  on the critical isotherm were computed from the equations of Hirschfelder *et al.* (HBMS), Martin & Hou (MH) and Benedict, Webb & Rubin (BWR).



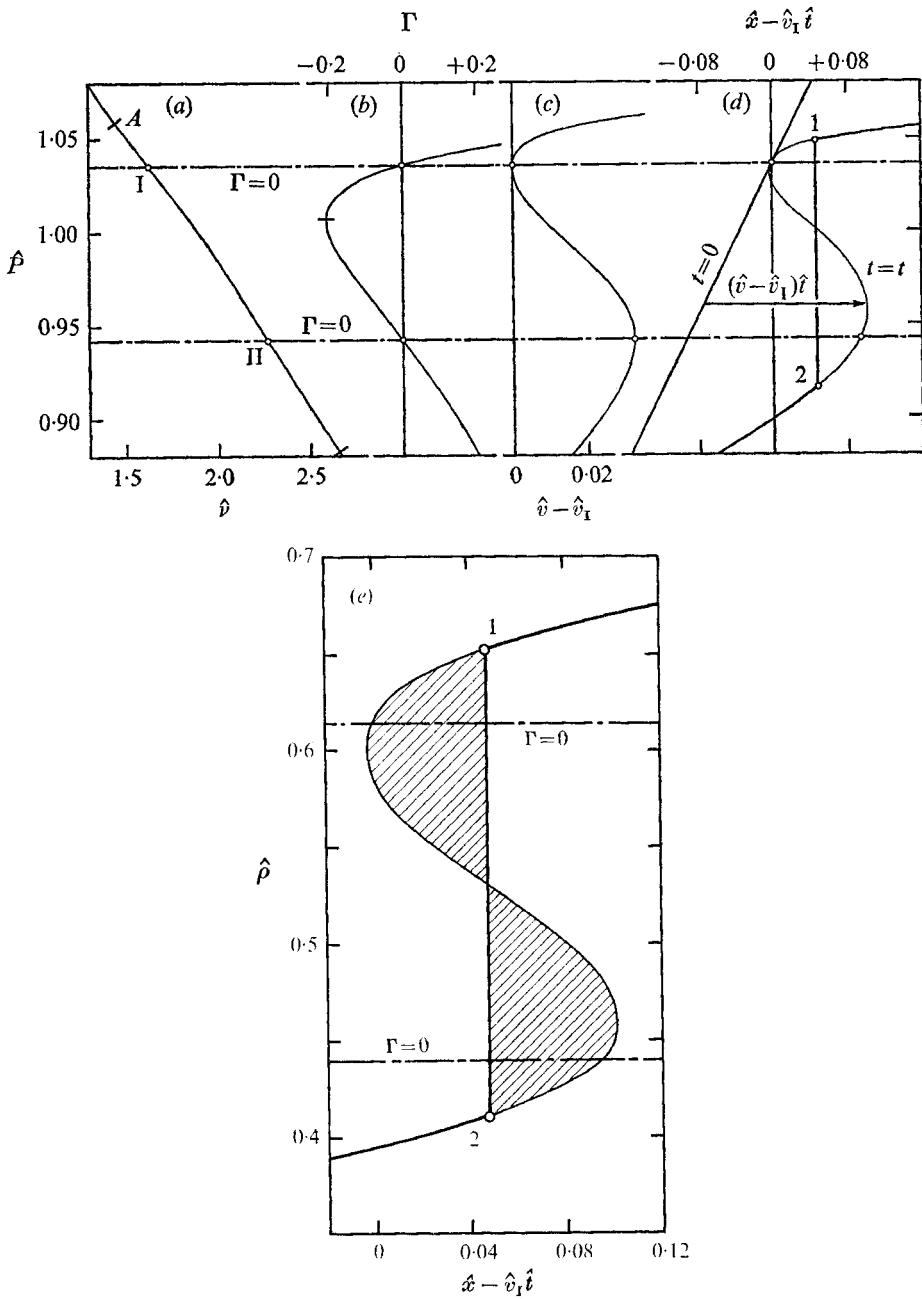


FIGURE 3. Wave distortion and negative shock formation, with representative hypothetical numerical values. (a) Isentrope in the  $P, v$  plane, with a negative- $\Gamma$  region between I and II. (b) Variation of  $\Gamma$  with  $P$ . (c) Variation of wave speed  $v$  with  $P$ . (d) Wave form  $P(x)$  at  $t = 0$  and  $t = t$ , after shock formation with fitted shock. (e) Shock fitting by conservation of mass, with equal shaded areas. The wave is travelling to the right.

We assume a simple wave, propagating in the  $+x$  direction into a uniform region. For (inviscid) homentropic flow, each local part of the wave travels with constant amplitude (e.g. pressure) at the local wave velocity  $v = u + c$ , where  $u$  is the fluid velocity and  $c$  is the sound speed. The progressive distortion of the wave is then completely determined by the manner in which  $v$  varies with amplitude. It is easy to show that  $v$  varies with pressure according to

$$dv/dP = \Gamma/\rho c. \quad (4.1)$$

An immediate consequence is that compression waves will steepen if  $\Gamma > 0$  and rarefaction waves will steepen if  $\Gamma < 0$ . The latter case is illustrated below.

A typical negative- $\Gamma$  region is shown in figures 3(a) and (b). The corresponding local wave velocity is found as a function of pressure by integration of (4.1):

$$v = \int \frac{\Gamma}{\rho c} dP + \text{constant}. \quad (4.2)$$

We note that the acoustic impedance  $\rho c$  is stationary in the vicinity of  $\Gamma = 0$  by virtue of (2.2), corresponding geometrically to a stationary value of the isentrope slope  $(\partial P/\partial v)_s$ ; thus (4.2) can be written as

$$v \approx \frac{1}{\rho c} \int \Gamma dP + \text{constant}. \quad (4.3)$$

This approximation will play no essential role in the following, but illustrates the progression from figure 3(b) to figure 3(c), where  $v(P)$  is shown. The distortion of an initially given rarefaction wave is shown in figure 3(d). The upper and lower extremes of pressure in the wave are assumed to fall well on either side of  $\Gamma < 0$ , i.e. the wave spans more than the negative- $\Gamma$  region. This is the most comprehensive case; other cases may be calculated similarly.

For convenience we take the non-dimensional variables

$$\begin{aligned} \hat{P} &\equiv P/P_c, & \hat{v} &\equiv v/(P_c \nu_c)^{\frac{1}{2}}, & \hat{p} &\equiv \nu/\nu_c, & \hat{x} &\equiv x/L, \\ \hat{\rho} &\equiv 1/\hat{v}, & \hat{t} &\equiv (P_c \nu_c)^{\frac{1}{2}} t/L, & \hat{c} &\equiv c/(P_c \nu_c)^{\frac{1}{2}}, \end{aligned} \quad (4.4)$$

where  $L$  is a characteristic length formed from some initial value  $(dP/dx)_*$  of the pressure gradient,  $L \equiv P_c/(dP/dx)_*$ . In figure 3 the progressive distortion of the wave is (arbitrarily) shown relative to the point I, where  $\Gamma = 0$ . Thus, for example, (4.2) is written as

$$\hat{v} - \hat{v}_I = \int_{\hat{P}_I}^{\hat{P}} \frac{\Gamma}{\hat{\rho} \hat{c}} d\hat{P}. \quad (4.5)$$

Consider two adjacent points at  $x$  and  $x+dx$  on the initial wave form, with corresponding velocities  $v$  and  $v+dv$ . The point behind will just overtake the point ahead (provided that  $dv < 0$ ) in a time interval  $t = -dx/dv$ . This is the time required for the wave front to become locally vertical, corresponding to the intersection of characteristics or shock formation. With (4.1), this  $t$  is

$$t_* = - \frac{\rho c}{\Gamma (dP/dx)_0}, \quad (4.6)$$

where  $(dP/dx)_0$  is the initial pressure gradient, while  $\rho c$  and  $\Gamma$  are the local thermodynamic properties and do not change with time. Apparently, a shock will first form where the right-hand side is a minimum (approximately, where  $-\Gamma(dP/dx)_0$  is a maximum). Let us denote the corresponding property values by subscript  $*$ : then with the dimensionless variables of (4.4), the shock formation time  $t_*$  is given by

$$\hat{t}_* = -\hat{\rho}_* \hat{c}_*/\Gamma. \tag{4.7}$$

The distance required for shock formation is  $x_* = v_* t_*$ , or to a rough approximation  $x_* \approx c_* t_*$ .

For  $\hat{t} > \hat{t}_*$  the wave front ‘breaks’ and becomes triple-valued. The shock front discontinuity is then fitted (in the isentropic approximation) according to the well-known area-matching rule from the conservation of mass:

$$\int_{-\infty}^{\infty} \hat{\rho} d\hat{x} = \text{constant}, \tag{4.8}$$

which leads to the construction shown in figure 3(e), where the upstream and downstream shock states are labelled 1 and 2 respectively. It is remarkable that these states move *outside the negative  $\Gamma$  region* I–II after a relatively short time, as illustrated in the figure. We thus find that negative shocks can extend over regions broader than the negative- $\Gamma$  region, but can only be initiated within a negative- $\Gamma$  region.

The maximum amplitude of the negative shock, corresponding to the behaviour of the wave as  $t \rightarrow \infty$ , can be found analytically (it should be noted that we still assume the amplitude of the initial rarefaction wave to be sufficiently large so that this in itself does not limit the growth of the shock). Let  $x_0(\rho)$  be the initial position of the wave front: at time  $t$  the position of the wave front is

$$x(\rho) = x_0(\rho) + v(\rho)t. \tag{4.9}$$

Now as  $t \rightarrow \infty$  the term  $x_0$  makes a negligible contribution to the shock-fitting integral (4.8). Thus we can write, for constant  $t$ ,  $dx = t dv$  and the shock-fitting integral becomes  $\int \rho dv = \text{constant}$ , which is exact in the limit. We express this condition as

$$\int_2^1 \rho dv = 0, \tag{4.10}$$

where the path of integration is as shown in figure 4. Geometrically, the integral expresses the equality of the area underneath (in a topological sense) the continuous  $\rho(v)$  curve to that underneath the curve after fitting the shock discontinuity: formally, it yields equality of the shaded areas shown. Making use of (4.1) and (2.1), integration yields

$$[(\partial P/\partial v)_s]_1 = [(\partial P/\partial v)_s]_2, \tag{4.11}$$

which is equivalent to  $\rho_1 c_1 = \rho_2 c_2$ . Now if the states 1 and 2 fall outside the negative- $\Gamma$  region, as is necessarily the case for large  $t$ , equation (4.11) uniquely fixes the positions of 1 and 2 on the isentrope shown in figure 3(b): specifically, these states fall at *A* and *B*, the points of tangency of a line drawn tangential to the two dips on the isentrope. These points are the limits for the shock amplitude.

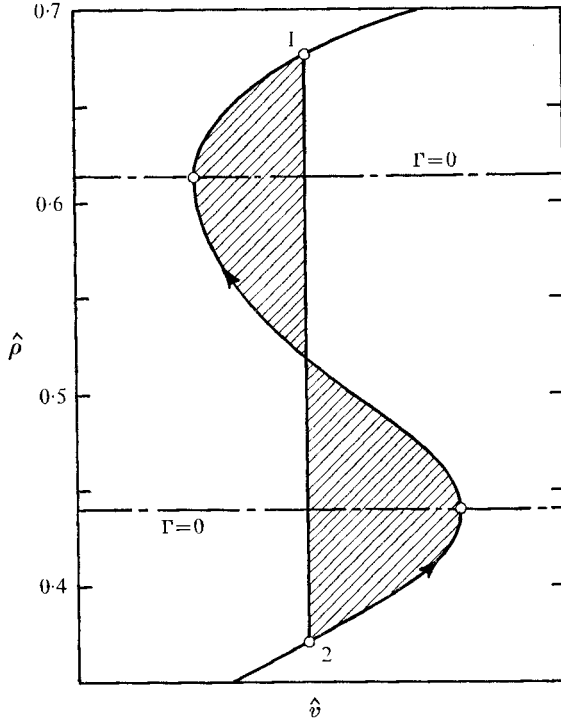


FIGURE 4. Asymptotic shock fitting for  $t \rightarrow \infty$ , with equal shaded areas.

An essential feature of the asymptotic construction shown in figure 4 is that the shock velocity  $V$  is equal to both the upstream and downstream wave velocities,  $V = u_1 + c_1 = u_2 + c_2$ . The fluid velocities relative to the shock front are then

$$w_1 = V - u_1 = c_1, \quad w_2 = V - u_2 = c_2 \tag{4.12}$$

and the Mach numbers relative to the shock front are unity;  $M_1 = M_2 = 1$ . The limiting shock then has the nature of a Chapman–Jouguet detonation wave, because  $M_2 = 1$ , but with the added feature that  $M_1 = 1$  also; thus it might be appropriate to call it a *double Chapman–Jouguet shock*. We comment further on this peculiar form of limiting shock in the following section.

We remark that this type of asymptotic limit on shock amplitude will never apply to an ideal gas or other substance in which  $v(\rho)$  is a monotonic function, i.e. in which  $\Gamma$  has the same sign everywhere. In these more typical cases, the shock amplitude will always be limited by the amplitude of the initial wave itself.

The above shock fitting is based on the isentropic assumption, which requires that the shock be weak. In the following section we show that this will almost always be the case for negative shocks.

### 5. Shock conditions

We take the shock to be a normal discontinuity stationary in our frame of reference, with velocities  $w_1$  and  $w_2$  into and out of the shock front, respectively. The basic jump equations for mass, momentum and energy respectively are

$$[\rho w] = 0, \tag{5.1}$$

$$[P + \rho w^2] = 0, \tag{5.2}$$

$$[h + \frac{1}{2}w^2] = 0, \tag{5.3}$$

where  $h$  is the specific enthalpy and the square bracket notation means  $[A] \equiv A_2 - A_1$ , where  $A$  is any quantity. On the basis of these equations and typical negative- $\Gamma$  behaviour, we wish to show that the conditions

$$[s] \geq 0 \tag{5.4}$$

and

$$M_1 \geq 1 \geq M_2 \tag{5.5}$$

can be satisfied for *negative* shock waves. The conditions (5.4) and (5.5) correspond respectively to the second law of thermodynamics and to shock stability, and are necessary for the existence and persistence of shocks. We remark that these conditions are easily met by negative shocks if  $\Gamma < 0$  everywhere (see, for example Thompson 1971); here, however, we want to allow the possibility that  $\Gamma$  changes sign once or twice along the shock adiabat, a situation which is likely to arise in real waves, as already indicated in §3.

Combination of (5.1)–(5.3) yields the alternative forms of the Rankine–Hugoniot relation

$$[h] = \frac{1}{2}(\nu_1 + \nu_2)[P], \quad [e] = -\frac{1}{2}(P_1 + P_2)[\nu], \tag{5.6}$$

where  $e$  is the specific internal energy.

We define the *shock strength*  $\Pi$ :

$$\Pi \equiv [P]/\rho_1 c_1^2. \tag{5.7}$$

For a positive shock  $\Pi > 0$ , for a negative shock  $\Pi < 0$ . If  $|\Pi|$  is small compared with unity, the shock may always be considered weak and the entropy jump will be negligible. In the case of a *negative* shock the shock may be considered weak in this sense even if  $|\Pi| \sim 1$ , as we verify below.

By Taylor expansion of  $h(P, s)$  about the upstream state **1**, making use of (5.6), one finds a series expression for the entropy jump:

$$T_1[s]/c_1^2 = \frac{1}{8}\Gamma_1 \Pi^3 + O(\Pi^4), \tag{5.8}$$

which is a form of Bethe’s equation (1.3). This indicates that the entropy jump is small for small  $\Pi$ , and that  $\Gamma$  and  $\Pi$  must have the same sign, since  $[s] > 0$ . For negative shocks with  $\Gamma_1 > 0$ , however, (5.8) does not even predict the correct sign for  $[s]$ ; a more satisfactory expression of (5.8) can be found using average values, assuming  $|\Gamma|$  small compared with unity:

$$\bar{T}[s]/c_1^2 \approx \frac{1}{8}\bar{\Gamma}\Pi^3 \dots, \tag{5.9}$$

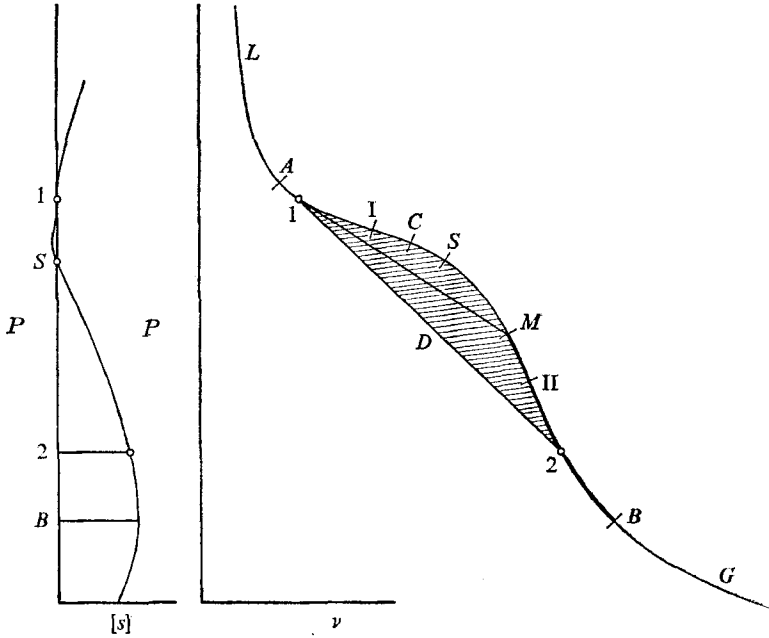


FIGURE 5. Shock adiabat for a negative shock with  $\Gamma_1 > 0$ . The interval of possible downstream states is between  $M$  and  $B$ . The various points of the adiabat are:  $L$ , liquid-like states;  $G$ , gas-like states;  $A$ , limiting upstream state;  $1$ , upstream state;  $I$ , inflexion point,  $\Gamma \approx 0$ ;  $C$ , Chapman–Jouguet point, where  $M_2 = 1$ ;  $S$ , point at which  $[s] = 0$ ;  $M$ , point at which  $M_1 = 1$ ;  $II$ , inflexion point,  $\Gamma \approx 0$ ;  $2$ , downstream state;  $B$ , limiting downstream state, also a Chapman–Jouguet point. The shaded area is equal to  $\bar{T}_{ad}[s]$ . Entropy distribution along the adiabat is shown at the left.

where

$$\bar{T} \equiv T_1 + \frac{1}{2}(\partial T / \partial P)_{s1}[P],$$

$$\bar{\Gamma} \equiv \frac{1}{[P]} \left[ \int_{P_1}^{P_2} \Gamma dP \right]_{s=s_1}.$$

We remark that the non-dimensional quantities  $\Pi$  and  $T[s]/c_1^2$  can be interpreted physically for weak shocks with  $M_1 \sim 1$ :  $\Pi$  is approximately that fraction of the upstream momentum flux which is converted to a pressure jump, while  $T[s]/c_1^2$  is approximately half the fraction of the upstream kinetic energy which is dissipated within the shock.

The shock adiabat formally given by (5.6) is shown in figure 5. If the isentrope passing through the upstream state  $1$  exhibits reversed curvature ( $\Gamma < 0$ ), it can be shown that the adiabat will also exhibit reversed curvature, as shown in the figure. In practice, the isentrope and adiabat can be taken as coincident over the possible negative shock range, as shown below.

For comprehensiveness, we have illustrated the case in which the upstream state  $1$  lies in a  $\Gamma > 0$  region. From the shock equations (5.1) and (5.2), the mass flux  $J \equiv \rho w$  through the shock is given by

$$J^2 = -[P]/[\nu], \tag{5.10}$$

which represents the slope of a chord drawn between state 1 and a downstream state 2 anywhere on the adiabat. The entropy variation  $ds = d(s - s_1)$  along the adiabat is given by

$$T ds = \frac{1}{2}(\nu - \nu_1) dJ^2, \tag{5.11}$$

found by Landau & Lifshitz (1959, p. 325). From this equation we infer the qualitative behaviour of the entropy along the adiabat, as shown in figure 5. There are three Chapman–Jouguet points (where the entropy is stationary,  $ds = 0$ ), namely point 1 and the two points at which the chord drawn from point 1 is tangential to the adiabat, points *C* and *B*.† At point *S*, where  $[s] = 0$ , it can be shown that  $(\partial P/\partial \nu)_s \approx (\partial P/\partial \nu)_{s1}$ . Downstream states to the left of *S* are ruled out by the second law.

For the calculation of the entropy jump  $[s]$ , a useful alternative to (5.9) is based on the overall geometry of the adiabat. Consider an integration around the closed path *1D2S1* in figure 5. From the Gibbs equation  $de = T ds - P d\nu$  we have at once

$$T ds = \oint P d\nu. \tag{5.12}$$

Making use of the Rankine–Hugoniot equation (5.6) this yields

$$\bar{T}_{ad}[s] = - \oint P d\nu, \tag{5.13}$$

where  $\bar{T} \equiv \int T ds/[s]$  is an average along the adiabat and the right-hand side corresponds to the shaded area shown in figure 5.

We now apply (5.13) to the estimation of the entropy jump across a negative shock wave of maximum amplitude, that is, a double Chapman–Jouguet wave extending between *A* and *B*. The problem of estimating  $\bar{T}_{ad}[s]$  in (5.13) is a geometrical one, that of finding the area between the undular adiabat and the tangent drawn from *A* to *B*. If the perpendicular distance between the chord *AB* and the adiabat is assumed to vary sinusoidally with distance along the adiabat, and the adiabat is treated as nearly coincident with the isentrope, one finds formally

$$\bar{T}_{ad}[s]/c_1^2 \approx (2\pi^2)^{-1} \Gamma_{\min} \Pi^3, \tag{5.14}$$

where  $\Gamma_{\min}$  is identified with the point of maximum distance between the chord and the adiabat. We remark that the right-hand side as written is not just the first term of a series, and is not restricted to small values of  $|\Pi|$ .

We can now estimate the degree of coincidence between the adiabat and the isentrope passing through state 1. At any fixed pressure *P* the displacement  $\Delta\nu$  of the adiabat from the isentrope is  $\Delta\nu \approx (\partial\nu/\partial s)_p [s]$ . With  $T \sim T_c$ ,  $c_1^2 \sim (P_c \nu_c)^{\frac{1}{2}}$  and making use of thermodynamic identities, this yields

$$\Delta\nu/\nu \sim \epsilon Z_c (\bar{T}[s]/c_1^2). \tag{5.15}$$

An extreme numerical value corresponds to a double Chapman–Jouguet shock with  $\epsilon \sim 10^{-2}$ ,  $\Gamma_{\min} \sim -0.2$  and  $\Pi \sim -1$ , yielding  $\bar{T}[s]/c_1^2 \sim 10^{-2}$  and a negligible displacement  $\Delta\nu/\nu \sim 10^{-4}$ .

† Points *A* and *B* can be defined in the same sense as in § 4. In that case, *B* is strictly at the Chapman–Jouguet point only if the upstream state 1 is at *A*.

The stability requirement (5.5) remains to be discussed. If  $\Gamma$  changes relatively little between the upstream and downstream states we can use the relations

$$M_1 = 1 + \frac{1}{2}\Gamma_1\Pi \dots, \quad (5.16)$$

$$M_2 = 1 - \frac{1}{2}\Gamma_1\Pi \dots, \quad (5.17)$$

which are comparable to (5.8) and can be found by suitable Taylor expansions of the jump equations (Thompson 1972, p. 572). For positive shocks with  $\Gamma_1 > 0$  and negative shocks with  $\Gamma_1 < 0$ , these relations satisfy the requirement  $M_1 \geq 1 \geq M_2$ . However for positive shocks with  $\Gamma_1 < 0$  and for negative shocks with  $\Gamma_1 > 0$ , these relations (incorrectly, in general) contradict the stability requirement. We can, however, examine the behaviour of  $M_1$  and  $M_2$  in terms of the geometry of the shock adiabat, see figure 5. Since the entropy is stationary at the origin, the slope of the adiabat at 1 is  $(\partial P/\partial v)_{s1} = -\rho_1^2 c_1^2$ . The slope of the chord drawn from 1 to an arbitrary point 2 is, from (5.10),  $[P]/[v] = -\rho_1^2 w_1^2$ . Since  $(\partial P/\partial v)_{s1} > [P]/[v]$  for points beyond  $M$  we have  $w_1 > c_1$  or  $M_1 \geq 1$  for points from  $M$  to  $B$  and similarly  $M_1 < 1$  for points from 1 to  $M$ . Proceeding similarly for  $M_2$ , and assuming that the adiabat is geometrically coincident with the isentrope, we find that  $M_2 \leq 1$  for points from  $C$  to  $B$ , where point  $C$  is defined by

$$[P]/[v] = dP/dv = (\partial P/\partial v)_s,$$

and  $M_2 \geq 1$  for points from 1 to  $C$ . Thus we find that the stability requirement  $M_1 \geq 1 \geq M_2$  is satisfied for all downstream states 2 between  $M$  and  $B$ . It appears that the region for which this requirement is satisfied is always smaller than that for which  $[s] \geq 0$ .

The Mach numbers  $M_1$  and  $M_2$  can be conveniently related to the geometry of the (nearly isentropic) adiabat by a simple equation. The continuity condition (5.1) is  $\rho w = \text{constant}$ ; with  $M \equiv w/c$  and  $c^2 = -v^2(\partial P/\partial v)_s$  this can be written as

$$M^2(\partial P/\partial v)_s = \text{constant}. \quad (5.18)$$

An immediate consequence is that  $|(\partial P/\partial v)_s|_2 \geq |(\partial P/\partial v)_s|_1$ .

In the case of a double Chapman–Jouguet shock (which for conciseness we will call a CJ 2 shock) extending from  $A$  to  $B$  the entropy is stationary at both end points and the adiabat geometry yields

$$M_1 = 1 = M_2 \quad (5.19)$$

independently of any assumption of small entropy jump. This corresponds to the limiting shock already found in § 4. We remark that the parameter  $M_1^2 - 1$ , sometimes employed as a measure of shock strength, is not a good measure for the strength of a negative shock, since the parameter is zero for a maximum amplitude shock! For negative shocks in general, the shock Mach number  $M_1$  will usually be close to unity, because the isentrope (negative) curvature is slight. The general shock relation  $M_1^2[v]/v_1 = -\Pi$ , which can be derived from the basic jump equations (5.1) and (5.2), then gives

$$[v]/v_1 \approx -\Pi, \quad (5.20)$$

which is an exact equality in the case of a double Chapman–Jouguet wave.



To verify the validity of the isentropic approximation (i.e. treating the adiabat and isentrope as coincident) and to test estimates such as (5.14), we have made exact calculations for various shocks in a van der Waals substance with constant specific heat  $c_v$ . The internal energy  $e$  and  $s$  are given by, in reduced form,

$$\frac{e}{P_c v_c} = \frac{8c_v}{3R} \hat{T} - \frac{3}{\hat{p}} + \text{constant}, \tag{5.21}$$

$$\frac{s-s_c}{R} = \frac{c_v}{R} \ln \hat{T} + \ln \frac{3\hat{p}-1}{2}. \tag{5.22}$$

With (5.21) and (3.3), the Rankine–Hugoniot equation (5.6) can be written as an explicit formula  $\hat{P}_2(\hat{v}_2)$  for the shock adiabat:

$$\hat{P}_2 = \frac{\hat{P}_1 \left\{ \hat{v}_1 + \frac{1}{2}\epsilon(\hat{v}_1 - \hat{v}_2) - \frac{1}{3} \right\} + \left( \frac{1}{\hat{v}_1} - \frac{1}{\hat{v}_2} \right) \left\{ 3(1-\epsilon) - \frac{1}{\hat{v}_1} - \frac{1}{\hat{v}_2} \right\}}{\hat{p} + \frac{1}{2}\epsilon(\hat{v}_2 - \hat{v}_1) - \frac{1}{3}}, \tag{5.23}$$

where  $\epsilon = R/c_v = k - 1$  as before.

It is expected that the adiabat given by (5.23) will be nearly coincident with the isentrope  $\hat{P}_2(\hat{v}_2)$  given by (3.6). As an example, for the case  $\epsilon = \frac{1}{50}$  a typical CJ 2 shock has the following upstream (1) and downstream (2) properties:

$$\begin{aligned} \hat{P}_1 &= 1.0532, & \hat{v}_1 &= 0.9841, & \hat{T}_1 &= 1.0187, \\ \hat{P}_2 &= 0.7964, & \hat{v}_2 &= 2.2036, & \hat{T}_2 &= 0.9919, \\ (s_2 - s_1)/R &= 0.00260. \end{aligned}$$

By comparison, the isentropic downstream pressure  $\hat{P}(\hat{v}_2, \hat{s}_1)$  is 0.7963, which differs negligibly from the  $\hat{P}_2$  value on the adiabat, given above. The entropy jump in the form  $\bar{T}[s]/c_v^2$  is 0.0342: by comparison, the value estimated by (5.14), with  $\Gamma_{\min} = -0.66$  and  $\Pi = 1.239$ , is 0.063, i.e. the estimate is too large by about a factor of two. It is interesting to note that the temperature jump  $[\hat{T}] = -0.0268$ , corresponding to a dimensional jump, for a fluid with (say)  $T_c = 600 \text{ K}^\circ$ , of  $-16 \text{ }^\circ\text{K}$ . While the preceding results are exaggerated by the tendency of the van der Waals equation to yield extreme negative- $\Gamma$  values, they can be taken to be indicative of actual behaviour.

The shock existence problem may be put as follows: given an upstream state 1, we define a *proper downstream state* 2 as one which satisfies the conditions (5.4)–(5.6). In practice, a proper negative-shock downstream state exists for nearly any upstream state lying between points *A* and *II* on an isentrope (figure 5). For an upstream state between *I* and *II* (i.e. with  $\Gamma_1 < 0$ ) the qualifier ‘nearly’ may be removed; if the upstream state lies between *A* and *I* (i.e. with  $\Gamma_1 > 0$ ), the existence of a proper downstream state involves some relation between  $(\partial^2 P/\partial v^2)_s$  and  $(\partial P/\partial s)_v$ , which we shall not pursue, this problem having been briefly discussed by Kline & Shapiro (1953).

## 6. Remarks on shock structure

The physical reality of negative shock waves can be made more plausible by the discovery of an internal structure consistent with the Navier–Stokes equations. By using weak-shock approximations, results can be obtained in simple algebraic form.

The shock is assumed to be steady and one-dimensional in a wave reference frame with space co-ordinate  $x$ . There is a uniform upstream state 1 at  $x = -\infty$  and uniform downstream state 2 at  $x = +\infty$ . The one-dimensional Navier–Stokes equation has a first integral

$$\rho u^2 + P - \frac{4}{3}\mu' \frac{du}{dx} = \rho_1 u_1^2 + P_1, \quad (6.1)$$

where  $\mu' \equiv \mu + \frac{3}{4}\mu_\nu$  is a combination of the shear viscosity  $\mu$  and bulk viscosity  $\mu_\nu$ , and  $\rho u = \rho_1 u_1 = \text{constant}$ .

To reduce this to a differential equation in  $u(x)$ , we expand  $P(v, s)$  in a Taylor series

$$P - P_1 = \left(\frac{\partial P}{\partial v}\right)_s (v - v_1) + \frac{1}{2} \left(\frac{\partial^2 P}{\partial v^2}\right)_s (v - v_1)^2 \dots + \left(\frac{\partial P}{\partial s}\right)_v (s - s_1) \dots, \quad (6.2)$$

where  $v - v_1 = v_1(u/u_1 - 1)$  by continuity. It is desired to retain terms up to  $(v - v_1)^2$  and thus obtain a ‘second-order’ theory. While the overall entropy change  $[s]$  is of third order in  $[\nu]$ , the entropy will have an extremum inside the shock front and retention of the entropy term in (6.2) will yield a second-order term. Writing  $s - s_1 = \int (ds/dx) dx$  and finding the integrand from the entropy production, viz.

$$\rho u T \frac{ds}{dx} = \frac{4}{3}\mu' \left(\frac{du}{dx}\right)^2 + \kappa \frac{d^2 T}{dx^2}, \quad (6.3)$$

yields

$$s - s_1 \approx \frac{\kappa v_1}{u_1 T_1} \frac{dT}{dx}, \quad (6.4)$$

where the viscosity  $\mu'$  and thermal conductivity  $\kappa$  have been assumed constant and the viscous dissipation term in (6.3) has been dropped, because it is small compared with the heat-conduction term if  $(\mu' c_p / \kappa) M_1^2 [\nu] / \nu_1 \ll 1$ , or more simply, if  $[\nu] / \nu_1 \ll 1$ . Writing  $T - T_1 \approx (\partial T / \partial v)_s (v - v_1)$ , and making use of the continuity equation and thermodynamic identities, the differential equation (6.1) becomes

$$(M_1^2 - 1) U + \Gamma U^2 = \alpha (dU/dX), \quad (6.5)$$

where  $M_1$  has been assumed near unity and

$$U \equiv (u - u_1)/u_1, \quad X \equiv \rho_1 c_1 x / \mu, \\ \alpha \equiv \frac{4}{3} + \mu_\nu / \mu + (\gamma - 1) / Pr.$$

The quantity  $\alpha$  is the non-dimensional form of the Kirchoff diffusivity. The differential equation (6.5) was found independently, but an equivalent form was given earlier by Hayes (1958).

Equation (6.5) has a solution

$$\ln \left[ \frac{-\Gamma U}{M_1^2 - 1 + \Gamma U} \right] = \frac{M_1^2 - 1}{\alpha} X, \quad (6.6)$$

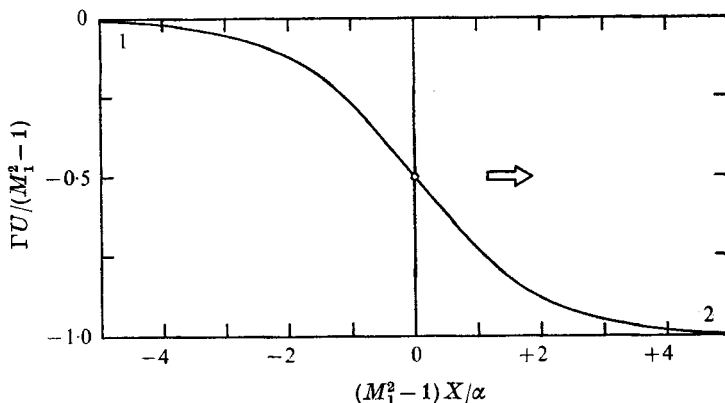


FIGURE 6. Velocity distribution across a weak shock, non-dimensional co-ordinates.

which is plotted in figure 6. This is a shock-type solution over the interval

$$0 \geq \Gamma U / (M_1^2 - 1) \geq -1$$

and it is easy to verify that this corresponds to either positive shocks ( $\Gamma > 0, U \leq 0$ ) or negative shocks ( $\Gamma < 0, U \geq 0$ ).

For a *perfect gas* we put  $\Gamma = \frac{1}{2}(\gamma + 1)$  in (6.6) which, after setting

$$M_1^2 - 1 \approx 2(M_1 - 1),$$

reduces to the famous solution of Taylor (1910) as discussed by Lighthill (1956).

The shock thickness is easily calculated. To show explicitly the influence of  $\Gamma$ , we write (5.16) in the form

$$M_1^2 - 1 \approx \Gamma \Pi.$$

If the shock thickness  $\Delta$  is arbitrarily taken to extend over a non-dimensional distance  $(M_1^2 - 1) \Delta X / \alpha = 10$ , corresponding to 98.7% of the overall velocity change, we obtain  $\Delta X = 10\alpha / (\Gamma \Pi)$  or a dimensional thickness

$$\Delta = \frac{10\alpha}{\Gamma \Pi} \frac{\mu}{\rho_1 c_1}. \tag{6.7}$$

The quantity  $\mu / (\rho_1 c_1)$  has dimensions of length and may be considered an effective mean free path (note, however, that at the requisite densities molecules interact more-or-less continuously). A typical value for  $\mu / (\rho_1 c_1)$  is roughly  $10^{-9}$  m. There is considerable question about the value of  $\alpha$ , because of uncertainty about  $\mu_v$ , but as a guess we can take  $\alpha = 2$ . Then for a representative negative shock with  $\Gamma = -0.1$  and  $\Pi = -0.2$  we obtain a shock thickness  $\Delta \approx 10^{-6}$  m.

Note that the shock thickness given by (6.7) depends inversely on  $\Gamma$ . While the solution given here cannot account for the variation of  $\Gamma$  with pressure, it is reasonable that the very small *average* values of  $\Gamma$  in negative shocks will correspond to a thick shock structure, even though  $\Pi$  may be of order unity. It is also remarked that the theory given in §4 predicts that waves cannot deform in (hypothetical) fluids with  $\Gamma = 0$  and shocks will not form: this seems consistent with (6.7), which predicts infinite thickness for a 'shock' in such a fluid!

We offer a few comments on the possibility that the shock is either partly or fully dispersed by vibrational relaxation of the complex molecules necessarily composing the fluid. For the estimated shock thickness  $\Delta \sim 10^{-6}$  m and a sound speed  $c \sim 40$  m/s, the fluid has a residence time  $\tau_s$  within the shock given by  $\tau_s \sim 2 \times 10^{-8}$  s. We can compare  $\tau_s$  with the vibrational relaxation time  $\tau$ : if  $\tau \ll \tau_s$ , the equilibrium viscous shock structure is appropriate, vibrational relaxation effects being incorporated into the bulk viscosity. The relaxation time  $\tau = 1/pZ$ , where  $p$  is the probability of excitation and  $Z$  is the collision frequency. According to Landau–Teller theory the dominant dependence of  $p$  is expressed by  $\log p \propto -\omega^2$ , where  $\omega$  is the minimum vibrational frequency, a result nicely substantiated by the Lambert–Salter plot of  $\log(1/p)$  versus  $\omega$  from experimental data (Lambert 1972). The minimum frequency  $\omega$  tends to decrease with molecular complexity. Although few data are available for highly complex molecules, we can give values (in spectroscopic notation) for *n*-pentane ( $149 \text{ cm}^{-1}$ ) and hexafluorobenzene ( $175 \text{ cm}^{-1}$ ). Making use of the latter figure, the Landau–Teller theory yields a relaxation time for hexafluorobenzene  $\tau = 10^{-10}$  s. For other substances considered one obtains similar values, the smallness of  $\tau$  being attributed to the large collision frequencies (at the high densities involved) and small fundamental frequencies. It thus appears that negative shocks may not be dispersed by relaxation, especially since the substances mentioned above are probably insufficiently complex to yield negative- $\Gamma$  behaviour.

## 7. Concluding remarks

That negative shocks may be found in experiments with vapour-phase fluids is suggested by the foregoing. Certain practical difficulties, including the appearance of critical phenomena, thermal stability of working fluids and the adequacy of existing equation-of-state information may be raised, however. We briefly discuss these questions in turn.

The immediate vicinity of the critical point is marked by departures from the behaviour predicted by any ‘classical’ equation of state, notably a sharp increase in the value of  $c_v$ , by changes in the transport properties, by random fluctuations in density and by the appearance of strong thermal–gravity convection (because  $\partial v/\partial T \rightarrow \infty$ ). These peculiar phenomena may strongly influence wave propagation. By virtue of the classical predictions of §3 it appears that negative-shock experiments can be carried out sufficiently far from the critical point so that anomalies will not arise, i.e. because the  $\Gamma < 0$  region extends far from the critical point. The central question for present purposes is: how large is the ‘critical region’? To oversimplify, we can arbitrarily put the critical region between  $\hat{p} = 0.85$  and  $\hat{p} = 1.15$ , and between the isotherms  $\hat{T} = 0.99$  and  $1.01$ : that is, non-classical behaviour is essentially confined to this region. Then most or all of the  $\Gamma < 0$  region falls outside the critical region (see figure 2). Of course, certain quantities are still large outside the above-defined critical region, in particular the volume expansion  $(\partial v/\partial T)_p$ . To test the importance of the gravity–convection (body-force) term in the equation of motion, we find the ratio of the ‘buoyancy force’  $g(\rho_0 - \rho)$  to the wave pressure-gradient term  $\nabla P$ . Using the van der Waals

equation, with a wave pressure gradient  $|\nabla P| \sim P_c \text{ m}^{-1}$  and a temperature fluctuation  $\Delta T \sim 1^\circ\text{K}$ , we find this ratio  $< 10^{-3}$  for  $\hat{p} > 1.2$ . It appears therefore that difficulties with critical phenomena may be avoided.

As molecular complexity increases, so does the tendency toward thermal decomposition. From the standpoint of stability near the critical temperature and large  $c_v/R$ , the fully fluorinated cyclic and aromatic compounds are attractive: for example, substances such as perfluorodecalin and decafluorobiphenyl are promising for experiments. In practical application, thermal stability can be improved by purification, degassing and use of inert vessels. It appears that there are available substances of adequate stability with  $c_v/R$  as large as 100.

As may be apparent from §3 of this paper, the accurate prediction of the crucial parameter  $\Gamma$  from empirical equation-of-state information is a major difficulty. While it appears that  $\Gamma$  does become negative at a sufficiently large value of  $c_v^0/R$ , just how large this value must be is uncertain (we should mention that the tendency towards  $\Gamma < 0$  is helped also by small values of the Riedel parameter  $\alpha_c$ ). This uncertainty is not surprising, since the calculation of a second derivative (i.e.,  $\partial^2 P/\partial v^2$ ) from any correlation of empirical data is a severe test of both the data and correlation. Fortunately,  $\Gamma$  can be measured experimentally and this provides both a stringent test of the equation-of-state information and a basis for its improvement. The determination of  $\Gamma$  can be made by means of sound speed measurements, or more directly by recording the distortion of a pressure pulse in a shock tube: if the local wave velocity  $v(P)$  is measured by means of two consecutive pressure transducers along the wave path, (4.1) yields a direct determination of  $\Gamma$ .

Finally, negative shocks with most of the properties discussed here have been observed in fused silica, an amorphous solid (Barker & Hollenbach 1970). In the  $\Gamma < 0$  region both the spreading of compression waves and steepening of rarefaction waves were observed. The shock adiabat is similar to figure 5.

The authors are pleased to acknowledge helpful discussions with Michael Abbott and the assistance of David Yaney in numerical computations.

#### REFERENCES

- ABBOTT, M. M. 1973 Cubic equations of state. *A.I.Ch.E. J.* (in press).
- BARKER, L. M. & HOLLENBACH, R. E. 1970 Shock-wave studies of PMMA, fused silica, and sapphire. *J. Appl. Phys.* **41**, 4208–4226.
- BETHE, H. A. 1942 The theory of shock waves for an arbitrary equation of state. *Office Sci. Res. & Dev., Washington, Rep.* no. 545.
- DUHEM, P. 1909 Sur la propagation des ondes de choc au sein des fluides. *Z. Phys. Chem., Leipzig*, **69**, 169–186.
- HATSOPoulos, G. N. & KEENAN, J. H. 1965 *Principles of General Thermodynamics*. Wiley.
- HAYES, W. D. 1958 The basic theory of gasdynamic discontinuities. In *Fundamentals of Gasdynamics* (ed. H. W. Emmons), pp. 416–481. Princeton University Press.
- HIRSCHFELDER, J. O., BUEHLER, R. J., MCGEE, H. A. & SUTTON, J. R. 1958 Generalized thermodynamic excess functions for gases and liquids. *Ind. Engng Chem.* **50**, 386.
- JOUGUET, E. 1901 Sur la propagation des discontinuités dans les fluides. *C.R. Acad. Sci., Paris*, **132**, 673–676.

- KLINE, S. J. & SHAPIRO, A. H. 1953 On the normal shock wave in any single-phase fluid substance. *Heat Transfer and Fluid Mechanics Institute*, pp. 193–210. Stanford University Press.
- LAMBERT, J. D. 1972 Vibration–translation and vibration–rotation energy transfer in polyatomic molecules. *J. Chem. Soc. Faraday Trans. 2* (II), 364–373.
- LAMBRAKIS, K. C. & THOMPSON, P. A. 1972 Existence of real fluids with a negative fundamental derivative  $\Gamma$ . *Phys. Fluids*, **15**, 933–935.
- LANDAU, L. D. & LIFSHITZ, E. M. 1959 *Fluid Mechanics*. Pergamon.
- LIGETHILL, M. J. 1956 Viscosity effects in waves of finite amplitude. In *Surveys in Mechanics* (ed. G. K. Batchelor & R. M. Davies), pp. 250–351. Cambridge University Press.
- MARTIN, J. J. & HOU, Y. C. 1955 Development of an equation of state for gases. *A.I.Ch.E. J.* **1**, 142.
- RANKINE, W. J. M. 1870 On the thermodynamic theory of waves of finite longitudinal disturbance. *Proc. Roy. Soc. A* **160**, 277–286.
- RAYLEIGH, LORD 1910 Aerial plane waves of finite amplitude. *Proc. Roy. Soc. A* **84**, 247–284.
- TAYLOR, G. I. 1910 The conditions necessary for discontinuous motion in gases. *Proc. Roy. Soc. A* **84**, 371–377.
- THOMPSON, P. A. 1971 A fundamental derivative in gasdynamics. *Phys. Fluids* **14**, 1843–1849.
- THOMPSON, P. A. 1972 *Compressible Fluid Dynamics*. McGraw-Hill.
- ZEL'DOVICH, YA. B. 1946 On the possibility of rarefaction shock waves. *Zh. Eksp. Teor. Fiz.* **4**, 363–364.
- ZEL'DOVICH, YA. B. & RAIZER, YU. P. 1966 *Physics of Shock Waves and High-Temperature Hydrodynamic Phenomena*, vol. 1 (ed. W. D. Hayes & R. F. Probstein), pp. 67–69. Academic.
- ZEL'DOVICH, YA. B. & RAIZER, YU. P. 1967 *Physics of Shock Waves and High-Temperature Hydrodynamic Phenomena*, vol. 2 (ed. W. D. Hayes & R. F. Probstein), pp. 757–762. Academic.
- ZEMPLÉN, G. 1905 Sur l'impossibilité des ondes de choc negatives dans les gaz. *C.R. Acad. Sci., Paris*, **141**, 710–712.